Genes, Brain and Behavior
Official publication of the International Behavioural and Neural Genetics Society

Genes, Brain and Behavior (2012) ***11:*** *62–68* doi: 10.1111/j.1601-183X.2011.00733.x

Preliminary evidence of abnormal white matter related to the fusiform gyrus in Williams syndrome: a diffusion tensor imaging tractography study

B. W. Haas[†], F. Hoeft[†], N. Barnea-Goraly[†], G. Golarai[‡], U. Bellugi[§] and A. L. Reiss[*,†]

[†]Department of Psychiatry and Behavioral Sciences, Center for Interdisciplinary Brain Sciences Research (CIBSR), Stanford University School of Medicine, Palo Alto, [‡]Department of Psychology, Stanford University, Palo Alto, and [§]Laboratory for Cognitive Neuroscience, Salk Institute for Biological Studies, La Jolla, CA, USA
**Corresponding author: A. L. Reiss, MD, Center for Interdisciplinary Brain Sciences Research, Stanford University School of Medicine, 401 Quarry Road, Stanford, CA 94305-5719, USA. E-mail: areiss1@stanford.edu*

Williams syndrome (WS) is a genetic condition caused by a hemizygous microdeletion on chromosome 7q11.23. WS is characterized by a distinctive social phenotype composed of increased drive toward social engagement and attention toward faces. In addition, individuals with WS exhibit abnormal structure and function of brain regions important for the processing of faces such as the fusiform gyrus. This study was designed to investigate if white matter tracts related to the fusiform gyrus in WS exhibit abnormal structural integrity as compared to typically developing (TD; age matched) and developmentally delayed (DD; intelligence quotient matched) controls. Using diffusion tensor imaging data collected from 40 (20 WS, 10 TD and 10 DD) participants, white matter fibers were reconstructed that project through the fusiform gyrus and two control regions (caudate and the genu of the corpus callosum). Macro-structural integrity was assessed by calculating the total volume of reconstructed fibers and micro-structural integrity was assessed by calculating fractional anisotropy (FA) and fiber density index (FDi) of reconstructed fibers. WS participants, as compared to controls, exhibited an increase in the volume of reconstructed fibers and an increase in FA and FDi for fibers projecting through the fusiform gyrus. No between-group differences were observed in the fibers that project through the control regions. Although preliminary, these results provide further evidence that the brain anatomy important for processing faces is abnormal in WS.

Keywords: DTI, fusiform, genetics, tractography, Williams syndrome

Received 17 June 2011, revised 19 August 2011, accepted for publication 9 September 2011

Introduction

Williams syndrome (WS) is a neurodevelopmental condition caused by a hemizygous microdeletion on chromosome 7q11.23. WS is characterized by a distinctive social phenotype characterized by hypersociability, social disinhibition and increased attention toward faces. For example, as compared to chronologically and mentally age-matched controls, individuals with WS rate photographs of facial expressions as more approachable (Jones *et al*. 2000), approach others such as strangers more frequently (Doyle *et al*. 2004), and fixate on faces longer (Riby *et al*. 2010). Together, these findings lend support to the hypothesis that WS is associated with abnormalities in brain regions important for social-cognitive functioning and in particular the processing of facial expressions (Martens *et al*. 2008).

One brain region particularly important for the processing of social information conveyed through facial expressions is the fusiform gyrus. The fusiform gyrus contains the fusiform face area (FFA), which is a highly specialized region for face recognition (Kanwisher *et al*. 1997). For example, BOLD activation within the FFA correlates with the ability to detect the presence of faces (Grill-Spector *et al*. 2004), and damage to the FFA, as in acquired prosopagnosia, results in a compromised ability to recognize facial expressions (Barton 2008). Recently, evidence has emerged that WS is associated with structural and functional abnormalities within the fusiform gyrus. Individuals with WS exhibit greater cortical gray matter thickness (Thompson *et al*. 2005) and reduced gray matter volume of the fusiform gyrus (Campbell *et al*. 2009) and greater volume of the functionally defined FFA within the fusiform gyrus (Golarai *et al*. 2010). In spite of evidence of structural and functional abnormalities within the fusiform gyrus in WS, very little is known regarding alterations of white matter related to the fusiform gyrus in WS.

This study was designed to investigate the integrity of white matter fibers that project through the fusiform gyrus in WS by using a diffusion tensor imaging (DTI) tractography approach. DTI is a neuroimaging technique that is particularly advantageous for elucidating the structural integrity of white matter within the living human brain based on measurements of water diffusion. DTI *tractography* integrates this information to infer connectivity patterns associated with *a*

© 2011 The Authors
Genes, Brain and Behavior © 2011 Blackwell Publishing Ltd and International Behavioural and Neural Genetics Society

priori defined regions of the brain (Lazar 2010). Thus, DTI tractography is a particularly useful tool to infer patterns of brain connectivity in both normal and pathological conditions.

On the basis of evidence that WS is associated with abnormalities in face processing (Karmiloff-Smith *et al*. 2004; Leonard *et al*. 2011) and with abnormalities in the gray matter structure (Campbell *et al*. 2009; Thompson *et al*. 2005) and function (Golarai *et al*. 2010) of the fusiform gyrus, we predicted that WS is associated with abnormalities in the white matter tracts related to the fusiform gyrus. We tested this hypothesis by reconstructing white matter fibers that project through the fusiform gyrus in a sample of WS subjects as compared to two control groups: typically developing (TD) and developmentally delayed (DD). To examine the anatomical specificity of white matter abnormalities in WS, we also reconstructed white matter fibers that project through two other regions; the caudate and the genu of the corpus callosum.

Methods

Participants

A total of 40 individuals, 20 WS, 10 TD and 10 DD, participated in this study. Twenty WS participants [9 females: mean age = 28.19, SD = 9.55; mean intelligence quotient (IQ) = 63.21; 18 right handed] were recruited. All genetic diagnoses were confirmed using florescent *in situ* hybridization probes for elastin, a gene consistently found in the microdeletion associated with WS. All participants exhibited the medical and clinical features of the WS phenotype, including cognitive, behavioral and physical profiles.

TD subjects were recruited locally (Palo Alto, CA, USA) and were financially compensated for their participation (10 total: 2 females; mean age = 27.77, SD = 9.53; mean IQ = 114.33; 10 right handed). TD subjects were screened for a history of psychiatric or neurologic problems using the Symptom Checklist-90-R (SCL-90-R; Derogatis 1977). All subjects had SCL-90-R scores that fell within one SD of a normative sample.

Criteria for the DD control group were met if participants' full-scale IQ fell below one SD of the norm and participants did not have the diagnosis of WS (10 total: 7 females; mean age = 23.71, SD = 5.30; mean IQ = 70.9; 8 right handed). Among the DD individuals, seven had idiopathic DD and three had a diagnosis of fragile X syndrome, Turner syndrome and velocardiofacial syndrome.

The WS group exhibited a lower mean full-scale IQ as compared to the TD group [$t(1, 28) = 8.83$, $P < 0.001$]. However, there was no statistically significant difference in the mean full-scale IQ between the WS and the DD groups [$t(1, 28) = 1.54$, $P = 0.14$]. Furthermore, there were no statistically significant differences in age between the WS and TD groups [$t(1, 28) = 0.11$, $P = 0.91$], the DD and WS groups [$t(1, 18) = 1.37$, $P = 0.18$] or the DD and TD groups [$t(1, 18) = 1.18$, $P = 0.25$]. Lastly, there was no significant difference in the proportion of females to males between groups [*chi-square* $(2, N = 40) = 5.05$, $P = .08$].

No participants had a contraindication for magnetic resonance imaging and written informed consent and/or assent were obtained from each participant. This study was approved by the Stanford University Administrative Panel on Human Subjects in Medical Research.

Image acquisition

Magnetic resonance images (MRIs) of each subject's brain were acquired at the Richard M. Lucas Center for Imaging (Stanford University, Palo Alto, CA, USA) using a 3T Signa LX (GE Medical Systems, Milwaukee, WI, USA). A DTI sequence was based on a single-shot spin-echo echoplanar imaging sequence with diffusion sensitizing gradients applied on both sides of the 180° refocusing pulse (Basser *et al*. 1994). Imaging parameters for the diffusion-weighted sequence were as follows: field of view (FOV), 24 cm; matrix size, 128 × 128 (33 slices); echo time (TE), 60.4 ms; repetition time (TR), 12 200 ms; 33 axial–oblique slices; and slice thickness, 3.8 mm/skip 0.4 mm. Diffusion gradient duration was O = 32 ms, and diffusion weighting was $b = 815$ s/mm^2. In addition, two reference measurements (b_0 scans) having no diffusion sensitizing gradients were performed and averaged for each slice. Diffusion was measured along 12 diffusion directions (six non-collinear directions: XY, XZ, YZ, −XY, −XZ and −YZ). To obtain an appropriate signal to noise ratio, this pattern was repeated six times for each slice, with the sign of all diffusion gradients inverted for odd repetitions. Data were then averaged across all six repetitions. To delineate regions of interest (ROIs) (seeds) used for fiber tracking, a high resolution, three-dimensional T1-weighted anatomic gradient, receptive field spoiled gradient scan (SPGR), MRI sequence with the following parameters was used: TR = 35 ms; TE = 6 ms; flip angle = 45°; number of excitations = 1; matrix size = 256 × 256; FOV = 24 cm^2; 124 contiguous slices of 1.5-mm thickness image was collected for each subject.

Image processing

Diffusion-weighted images were corrected for eddy current distortions and head motion using linear image registration (automated image registration algorithm) (Woods *et al*. 1998). Thereafter, DtiStudio (Jiang *et al*. 2006) (https://www.dtistudio.org/) was used. All individual images were visually inspected to discard slices with motion artifacts, and the remaining images were averaged for each slice. There were no statistical differences in the proportion of discarded slices between groups ($P > 0.10$). The pixel intensities of the multiple diffusion-weighted images were fitted to obtain all elements of the symmetric diffusion tensor. The diffusion tensors at each pixel were diagonalized to obtain pixel eigenvalues and eigenvectors. Fractional anisotropy (FA) maps, average non-diffusion-weighted images ($b = 0$ s/mm^2) were retained.

Diffusion tensor fiber tracking

Fiber tracking was performed using the fiber assignment by continuous tracking method (Mori *et al*. 1999). Briefly, tracing was initiated from a seed voxel from which a line was propagated in both retrograde and orthograde directions according to eigenvector (v1) at each voxel. The tracking was terminated when it reached a voxel with an FA value lower than 0.15 (Wakana *et al*. 2004), or when the turning angle was greater than 70° (Roberts *et al*. 2005). To reconstruct branching patterns, the tracking was performed from every voxel inside the brain, but only fibers that penetrated *a priori* defined ROIs were retained.

Fusiform ROIs were outlined manually by reliable raters (intraclass interrater reliability >0.9), on positionally normalized brain image stacks in a coronal orientation perpendicular to the horizontal plane defined by the anterior and posterior commissures. The definition of the fusiform gyrus ROI included the gray and white matter between the lateral occipitotemporal sulcus and the lateral bank of the collateral sulcus (Fig. 1a). The anterior extent of the fusiform gyrus was defined by the coronal slice that intersected the posterior edge of the amygdala. The posterior extent of the fusiform gyrus was defined by the last coronal slice that included a white matter tract (Duvernoy 1999).

As control regions, ROIs were delineated to encompass the left and right caudate and the genu of the corpus callosum. The caudate ROIs were delineated using a knowledge-driven algorithm to delineate the caudate nucleus for each participant (Xia *et al*. 2007). This method has been shown to be reliable and to produce volumes that are suitable to detect condition-specific alterations in volume and in white matter tracts related to the caudate (Haas *et al*. 2009). The genu ROI was delineated by using a standardized circle ROI with a diameter of 10 voxels. The ROI was positioned on each participant's most medial sagital slice using a color map (DTI data), where the entire corpus callosum was most clearly visualized in red.

Measurements of total, gray and white volumes were calculated for the fusiform and caudate ROIs. Gray and white matter tissue types

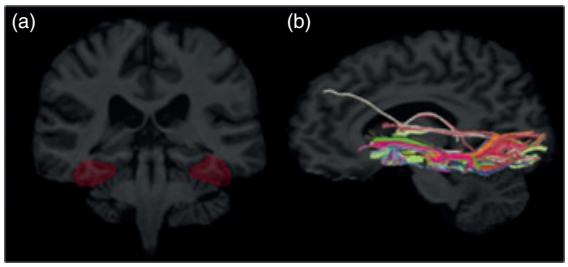

Figure 1: Fusiform gyrus ROIs (a) and reconstructed white matter fibers related to the fusifom gyrus (b) in one representative TD control subject. ROIs were delineated on each participant's high-resolution SPGR scan. The fusiform ROI included the gray and white matter between the lateral occipitotemporal sulcus and the lateral bank of the collateral sulcus. Fibers projecting through the fusiform gyrus are overlaid onto a high-resolution structural image 148 × 68 mm (72 × 72 DPI).

were segmented using a probabilistic tissue segmentation algorithm (Reiss *et al*. 1998) available within the program, BrainImage v5.x (Reiss 2010). The fusiform gyrus as defined in this study includes both gray and white matter, while the caudate is comprised almost entirely of gray matter. Therefore, for the fusiform gyrus, we separately entered gray and white matter as covariates into our statistical model, and for the caudate we entered total tissue volume as a covariate into our statistical model. We carried out these procedures to ensure that group differences in tissue volume were not affecting the DTI results.

The fusiform and caudate ROIs were aligned to DTI space by using a rigid body (affine) transformation. Spatial alignment was carried out by obtaining parameters derived from the coregistration from each participant's SPGR image to each participant's mean b_0 image (DTI data) and applying the parameters to each ROI.

Each ROI was used as a seed region in DTI space within DtiStudio (Fig. 1b). White matter fibers were selected if they projected through each *a priori* defined ROI (left and right fusiform gyrus, left and right caudate and genu). For each fiber tract bundle, metrics indicative of macro- and micro-structure were collected. Macro-structure was quantified by the total volume of each reconstructed fiber bundle. Micro-structure metrics included FA and fiber density index (FDi).

A priori statistical analyses were initiated by conducting a repeated measures analysis of variance (ANOVA) with group (WS vs. TD vs. DD) entered as a between-subjects factor and side (left vs. right, for fusiform and caudate) as the within-subjects factor. Each ANOVA comparing macro-structure was also conducted while controlling for total (caudate), gray (fusiform) and white (fusiform) matter volumes. Under the scenario that a significant effect of group was observed (WS vs. TD vs. DD), we examined main effects using each control group (WS vs. TD and WS vs. DD independently) and simple effects targeting each side (left and right independently) for each DTI metric.

Results

Fusiform: volume of reconstructed white matter tracts

Probabilistic maps of reconstructed white matter tracts for each group are shown in Fig. 2. We conducted a repeated measures ANOVA on the volume of reconstructed fibers that project through the fusiform with group (WS vs. TD vs. DD) as the between-subjects factor and hemisphere (left vs. right) as the within-subjects factor. This analysis showed a significant effect of group ($F_{2,37} = 7.091$, $P = 0.002$) and no significant effect of hemisphere ($F_{2,37} = 0.009$, $P = 0.92$) (Fig. 3a). The effect of group remained significant when gray and white matter ROI volumes were entered as covariates (gray: $F_{2,36} = 10.45$, $P < 0.001$ and white: $F_{2,36} = 7.00$, $P = 0.003$).

We next compared the volume of reconstructed fibers that project through the left and right fusiform independently between the WS group and each of the control groups. The WS group, as compared to the TD group, exhibited a greater volume of reconstructed fibers that project through the left [$t(1, 28) = 2.80$, $P < 0.01$] and right fusiform [$t(1, 28) = 2.39$, $P < 0.05$]. The WS group, as compared to the DD group, also exhibited a greater volume of reconstructed fibers that project through the left [$t(1, 28) = 2.74$, $P < 0.05$] and right fusiform [$t(1, 28) = 2.49$, $P < 0.05$]. No statistically significant difference in volume of reconstructed fibers that project through the fusiform was observed between the TD and DD control groups.

Fusiform: FA

We conducted a repeated measures ANOVA on the FA of reconstructed fibers that project through the fusiform with group (WS vs. TD vs. DD) as the between-subjects factor and hemisphere (left vs. right) as the within-subjects factor. This analysis showed a significant effect of group ($F_{2,37} = 3.97$, $P < 0.05$) and no significant effect of hemisphere ($F_{2,37} = 1.51$, $P = 0.23$) (Fig. 3b).

We next compared the FA of reconstructed fibers that project through the left and right fusiform independently between the WS group and each of the control groups. The WS group, as compared to the TD group, exhibited greater FA of reconstructed fibers that project through the left [$t(1, 28) = 2.09$, $P < 0.05$] and right fusiform [$t(1, 28) = 2.70$, $P < 0.01$]. However, the differences between the WS and DD groups did not reach statistical significance although the right side approached significance [left: $t(1, 28) = 1.03$, $P = 0.31$ and right: $t(1, 28) = 1.76$, $P = 0.09$]. No statistically significant difference in FA of reconstructed fibers that project through the fusiform was observed between the TD and DD control groups.

Fusiform: fiber density

For each fiber bundle, the mean number of reconstructed fibers per voxel was calculated (termed FDi). We conducted repeated measures ANOVA on the FDi of reconstructed fibers that project through the fusiform with group (WS vs. TD vs. DD) as the between-subjects factor and hemisphere (left vs. right) as the within-subjects factor. This analysis showed a significant effect of group ($F_{2,37} = 8.46$, $P = 0.001$) and no significant effect of hemisphere ($F_{2,37} = 0.88$, $P = 0.35$) (Fig. 3c).

We next compared the FDi of reconstructed fibers that project through the left and right fusiform independently between the WS group and each of the control groups. The WS group, as compared to the TD group, exhibited greater FDi of reconstructed fibers that project through the left [$t(1, 28) = 3.34$, $P < 0.005$] and right fusiform [$t(1, 28) = 2.06$, $P < 0.05$]. The WS group, as compared to the DD group exhibited greater FDi of reconstructed fibers that project through the left [$t(1, 28) = 3.00$, $P < 0.01$] and right fusiform [$t(1, 28) = 2.67$, $P < 0.05$]. No statistically

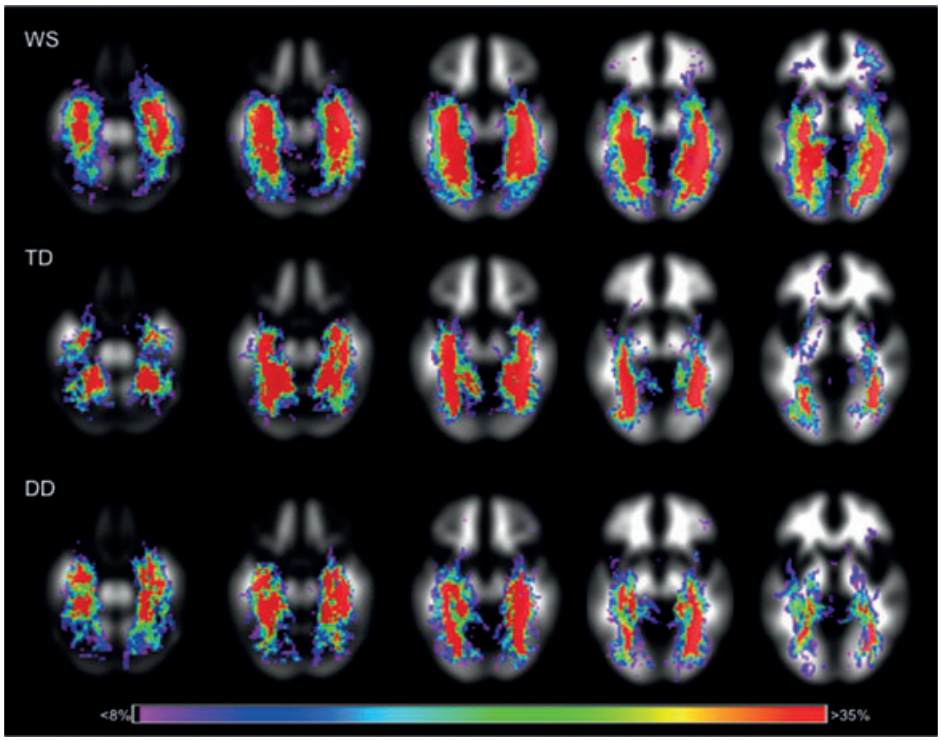

Figure 2: Probabilistic maps of reconstructed white matter fibers projecting through the fusiform gyrus in the WS ($N = 20$), TD ($N = 10$) and DD ($N = 10$) groups. Color scale corresponds to the relative probability of reconstructed fibers being present within each group 214 × 167 mm (72 × 72 DPI). Images are displayed in neurological convention (left side of the image corresponds to the left side of the brain).

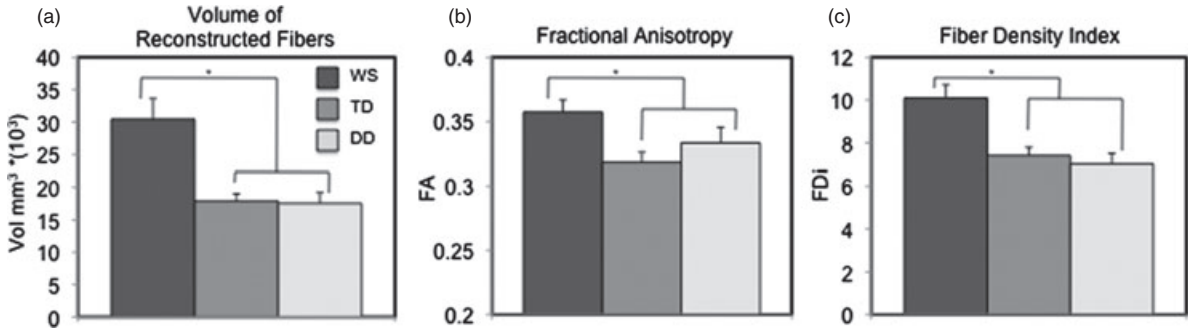

Figure 3: Plots of macro [(a) volume of reconstructed fibers] and micro [(b) FA and (c) FDi] for fibers projecting through the fusiform gyrus (averaged across left and right) in WS, TD and DD participants. Error bars represent standard error from the mean 250 × 79 mm (72 × 72 DPI). Vol (mm), volume in millimeters. *$P < 0.05$.

significant difference in FDi of reconstructed fibers that project through the fusiform was observed between the TD and DD control groups.

Control regions: all DTI metrics

We conducted repeated measures ANOVAs on each of the dependent variables (volume: controlling for caudate ROI total tissue volume, FA and FDi) related to the reconstructed fibers projecting through the caudate and the genu of the corpus callosum with group (WS vs. TD vs. DD) as the between-subjects factor and side (for the caudate) as the within-subjects factor. These analyses showed no significant effects of group or side for the caudate or the genu (all Ps > 0.10).

Discussion

In this study, we show that WS is associated with abnormal anatomy of white matter fibers projecting through the

fusiform gyrus. This finding is consistent with prior research showing that individuals with WS process facial expressions differently as compared to chronologically and mentally age-matched controls (Riby *et al*. 2010) and with prior research showing that WS is associated with alterations in gray matter structure (Campbell *et al*. 2009; Thompson *et al*. 2005) and function (Golarai *et al*. 2010) within the fusiform gyrus. Together, these studies indicate that WS may be associated with abnormal development of brain anatomy important for the processing of social information and in particular facial expressions.

This finding of abnormalities of white matter related to the fusiform gyrus may be an underlying neural substrate associated with the social phenotype of WS. As compared to TD controls, those with WS are less socially inhibited (Doyle *et al*. 2004), more attentive toward facial expressions (Riby *et al*. 2010) and more likely to rate facial expressions as being approachable (Bellugi *et al*. 1999). Recently, evidence has emerged suggesting that individuals with WS process faces differently as compared to controls. Specifically, those with WS tend to process faces based on individual features (i.e. eyes and mouth), while healthy controls process faces more holistically (i.e. the whole face combined) (Annaz *et al*. 2009; Isaac & Lincoln 2011; Karmiloff-Smith *et al*. 2004). Taken together, abnormal cognitive processing of faces, along with alterations of brain anatomy including the fusiform gyrus, likely interact and contribute to the WS social phenotype.

The fusiform gyrus exhibits extensive connections with many brain regions including visual processing areas, the frontal lobe and parietal lobe. The fusiform gyrus is also part of a distributed neural system that is highly specialized for face perception (Haxby *et al*. 2000). For example, the functional connectivity between the fusiform and the superior temporal sulcus and orbital frontal cortex is greater when healthy subjects view faces vs. scrambled images (Fairhall & Ishai 2007). In addition, Sarpal *et al*. (2008) showed that individuals with WS exhibit abnormal functional connectivity between the fusiform, amygdala and several portions of the prefrontal cortex during passive viewing of faces vs. houses. Our findings extend prior research by showing that the anatomical connections with the fusiform gyrus are structurally abnormal in WS.

In this study, we used a DTI tractography approach to measure white matter macro- and micro-structural integrity. Macro-structural integrity was assessed by calculating the total volume of reconstructed fibers. Micro-structural integrity was assessed by calculating FA and FDi. The metrics used here are most likely reflective of different neuroanatomical features. For example, the metric of macro-structure used here (the volume of reconstructed fibers) is not a direct measure of the real volume or number of axons within a particular tract. However, the volume of reconstructed fibers has been used to investigate white matter structural integrity in humans. For example, the volume of reconstructed fibers is reduced in clinical conditions characterized by white matter loss such as in cerebral palsy (Thomas *et al*. 2005) and in those affected by strokes (Schaechter *et al*. 2008). Further research combining DTI with functional neuroimaging techniques in humans and histological approaches in animals is necessary to elucidate the relationship between increased volume of fibers, functional anatomy and cytoarchitecture.

In terms of micro-structure, FA is a metric indicative of the proportion of linear diffusion (movement) of water molecules in a particular direction. Typically, locations composed of white matter tissue as compared to other types of tissues within the brain (i.e. gray matter) exhibit higher values of FA. FDi represents the average number of reconstructed fibers per voxel and is thought to be reflective of the density of white matter fibers projecting through a voxel (Roberts *et al*. 2005; Vernooij *et al*. 2007).

In this study, diffusion tensors were measured along 12 directions (six non-collinear directions). Recently, many DTI sequences have been designed to measure diffusion tensors along a greater number of directions relative to the data acquired for this study. Although it has been suggested that performing tractography with more diffusion directions is associated with a reduced likelihood of committing errors related to crossing or 'kissing' fibers, a direct comparison of the fidelity of diffusion-weighted data collected using optimized 6, 10, 15 and 30 direction schemes indicates that each has comparable precision and that they each have sufficient power to discriminate normal from abnormal white matter integrity (Landman *et al*. 2007). Furthermore, tractography analyses using diffusion-weighted data with six non-collinear directions have been shown to be effective in terms of dissociating white matter tracts related to autistic spectrum disorders (Sundaram *et al*. 2008), mental arithmetic skills (Tsang *et al*. 2009) and face perception (Thomas *et al*. 2008).

We observed statistically significant differences in both macro- and micro-structure between WS and controls. However, in terms of FA, we only observed statistically significant differences between the WS and TD groups and not between the WS and DD groups. The lack of a statistically significant difference in FA between the WS and DD groups may be due to several factors. For example, the DD group, as compared to the WS and TD groups, was relatively more heterogeneous. Among the DD individuals, seven had idiopathic DD and three had a non-WS diagnosis of fragile X syndrome, Turner syndrome and velocardiofacial syndrome. This study was also limited in terms of sample size for the DD group ($n = 10$). It may be the case that if there were a greater number of DD participants (as in the WS group), statistically significant differences may have been observed between the WS and DD group.

In this study, statistically significant differences were found between the WS and control groups in DTI metrics related to the fusiform gyrus, but not in DTI metrics related to other brain regions including the genu of the corpus callosum. Several studies have reported on structural abnormalities within the corpus callosum in WS, primarily in posterior regions such as the isthmus and splenium (Paul 2011). Our study used an approach to track white matter fibers related to the most anterior portion of the corpus callosum (genu). Clearly, more research on the structure and function of the corpus collosum in WS is warranted.

This findings presented here indicate that the deleted genes in WS may influence the development of the neuroanatomy involved in processing facial expressions. However, these results are based on data acquired from

adults with WS and thus are limited in terms of informing models of neurodevelopment in WS directly. Future studies designed to investigate neuro and behavioral development throughout early childhood in WS will help to elucidate the interaction between genes, environmental factors and social brain development in WS.

Although the results presented here highlight the presence of structural abnormalities of white matter associated with the fusiform gyrus in WS, these results must be taken as preliminary. Social functioning and in particular face processing is abnormal in WS. However, the fusiform gyrus is responsible for many functions (only one of which is face processing). Ideally, this study would have included behavioral data indicative of individual differences in face processing. However, these data were not acquired for a large enough subset within our sample, and thus statistical analyses were not justified. Another approach that would improve the specificity of these findings would be to acquire FFA localizer fMRI scans for each participant (Golarai *et al*. 2010). As a result, white matter tracts related to the face-processing region within the fusiform could be isolated more accurately. Accordingly, the results presented here should be considered preliminary and hypothesis generating with respect to further investigations of functional and structural aberrations of the fusiform gyrus in WS.

Conclusions

In conclusion, we have provided evidence that the white matter tracts associated with the fusiform gyrus exhibit abnormal macro- and micro-structural characteristics in WS as compared to chronologically and mentally age-matched controls. This finding provides further support for a model relating genetic risk in WS to structural and functional aberrations within the brain, ultimately influencing the development of distinctive social behaviors in this condition. Clearly, as behavioral and DTI approaches continue to advance, further research is warranted in this condition.

References

Annaz, D., Karmiloff-Smith, A., Johnson, M.H. & Thomas, M.S. (2009) A cross-syndrome study of the development of holistic face recognition in children with autism, Down syndrome, and Williams syndrome. *J Exp Child Psychol* **102**, 456–486.

Barton, J.J. (2008) Structure and function in acquired prosopagnosia: lessons from a series of 10 patients with brain damage. *J Neuropsychol* **2**, 197–225.

Basser, P.J., Mattiello, J. & LeBihan, D. (1994) MR diffusion tensor spectroscopy and imaging. *Biophys J* **66**, 259–267.

Bellugi, U., Adolphs, R., Cassady, C. & Chiles, M. (1999) Towards the neural basis for hypersociability in a genetic syndrome. *Neuroreport* **10**, 1653–1657.

Campbell, L.E., Daly, E., Toal, F., Stevens, A., Azuma, R., Karmiloff-Smith, A., Murphy, D.G. & Murphy, K.C. (2009) Brain structural differences associated with the behavioural phenotype in children with Williams syndrome. *Brain Res* **1258**, 96–107.

Derogatis, L.R. (1977) *SCL-90: administration, scoring and procedures manual for the revised version and other instruments of the psychopathology rating scale series*. John Hopkins University, Baltimore.

Doyle, T.F., Bellugi, U., Korenberg, J.R. & Graham, J. (2004) ''Everybody in the world is my friend'' hypersociability in young children with Williams syndrome. *Am J Med Genet A* **124**, 263–273.

Duvernoy, H. (1999) *The Human Brain*. Springer Wien, New York.

Fairhall, S.L. & Ishai, A. (2007) Effective connectivity within the distributed cortical network for face perception. *Cereb Cortex* **17**, 2400–2406.

Golarai, G., Hong, S., Haas, B.W., Galaburda, A.M., Mills, D.L., Bellugi, U., Grill-Spector, K. & Reiss, A.L. (2010) The fusiform face area is enlarged in Williams syndrome. *J Neurosci* **30**, 6700–6712.

Grill-Spector, K., Knouf, N. & Kanwisher, N. (2004) The fusiform face area subserves face perception, not generic within-category identification. *Nat Neurosci* **7**, 555–562.

Haas, B.W., Barnea-Goraly, N., Lightbody, A.A., Patnaik, S.S., Hoeft, F., Hazlett, H., Piven, J. & Reiss, A.L. (2009) Early white-matter abnormalities of the ventral frontostriatal pathway in fragile X syndrome. *Dev Med Child Neurol* **51**, 593–599.

Haxby, J.V., Hoffman, E.A. & Gobbini, M.I. (2000) The distributed human neural system for face perception. *Trends Cogn Sci* **4**, 223–233.

Isaac, L. & Lincoln, A. (2011) Featural versus configural face processing in a rare genetic disorder: Williams syndrome. *J Intellect Disabil Res* doi: 10.1111/j.1365-2788.2011.01426.x.

Jiang, H., van Zijl, P.C., Kim, J., Pearlson, G.D. & Mori, S. (2006) DtiStudio: resource program for diffusion tensor computation and fiber bundle tracking. *Comput Methods Programs Biomed* **81**, 106–116.

Jones, W., Bellugi, U., Lai, Z., Chiles, M., Reilly, J., Lincoln, A. & Adolphs, R. (2000) II. Hypersociability in Williams Syndrome. *J Cogn Neurosci* **12** (Suppl. 1), 30–46.

Kanwisher, N., McDermott, J. & Chun, M.M. (1997) The fusiform face area: a module in human extrastriate cortex specialized for face perception. *J Neurosci* **17**, 4302–4311.

Karmiloff-Smith, A., Thomas, M., Annaz, D., Humphreys, K., Ewing, S., Brace, N., Duuren, M., Pike, G., Grice, S. & Campbell, R. (2004) Exploring the Williams syndrome face-processing debate: the importance of building developmental trajectories. *J Child Psychol Psychiatry* **45**, 1258–1274.

Landman, B.A., Farrell, J.A., Jones, C.K., Smith, S.A., Prince, J.L. & Mori, S. (2007) Effects of diffusion weighting schemes on the reproducibility of DTI-derived fractional anisotropy, mean diffusivity, and principal eigenvector measurements at 1.5T. *Neuroimage* **36**, 1123–1138.

Lazar, M. (2010) Mapping brain anatomical connectivity using white matter tractography. *NMR Biomed* **23**, 821–835.

Leonard, H.C., Annaz, D., Karmiloff-Smith, A. & Johnson, M.H. (2011) Brief report: developing spatial frequency biases for face recognition in autism and Williams syndrome. *J Autism Dev Disord* **41**, 968–973.

Martens, M.A., Wilson, S.J. & Reutens, D.C. (2008) Research review: Williams syndrome: a critical review of the cognitive, behavioral, and neuroanatomical phenotype. *J Child Psychol Psychiatry* **49**, 576–608.

Mori, S., Crain, B.J., Chacko, V.P. & van Zijl, P.C. (1999) Three-dimensional tracking of axonal projections in the brain by magnetic resonance imaging. *Ann Neurol* **45**, 265–269.

Paul, L.K. (2011) Developmental malformation of the corpus callosum: a review of typical callosal development and examples of developmental disorders with callosal involvement. *J Neurodev Disord* **3**, 3–27.

Reiss, A.L., Hennessey, J.G., Rubin, M., Beach, L., Abrams, M.T., Warsofsky, I.S., Liu, A.M. & Links, J.M. (1998) Reliability and validity of an algorithm for fuzzy tissue segmentation of MRI. *J Comput Assist Tomogr* **22**, 471–479.

Reiss, A.L. (2010) BrainImage v5.x. Software Program. Center for Interdisicplinary Brain Sciences Research, Stanford University School of Medicine. URL http://www.cibsr.stanford.edu (Date of last access 20 February 2010).

Riby, D.M., Jones, N., Brown, P.H., Robinson, L.J., Langton, S.R., Bruce, V. & Riby, L.M. (2010) Attention to faces in Williams syndrome. *J Autism Dev Disord* **41**, 1228–1239.

Roberts, T.P., Liu, F., Kassner, A., Mori, S. & Guha, A. (2005) Fiber density index correlates with reduced fractional anisotropy in white matter of patients with glioblastoma. *Am J Neuroradiol* **26**, 2183–2186.

Sarpal, D., Buchsbaum, B.R., Kohn, P.D., Kippenhan, J.S., Mervis, C.B., Morris, C.A., Meyer-Lindenberg, A. & Berman, K.F. (2008) A genetic model for understanding higher order visual processing: functional interactions of the ventral visual stream in Williams syndrome. *Cereb Cortex* **18**, 2402–2409.

Schaechter, J.D., Perdue, K.L. & Wang, R. (2008) Structural damage to the corticospinal tract correlates with bilateral sensorimotor cortex reorganization in stroke patients. *Neuroimage* **39**, 1370–1382.

Sundaram, S.K., Kumar, A., Makki, M.I., Behen, M.E., Chugani, H.T. & Chugani, D.C. (2008) Diffusion tensor imaging of frontal lobe in autism spectrum disorder. *Cereb Cortex* **18**, 2659–2665.

Thomas, B., Eyssen, M., Peeters, R., Molenaers, G., Van Hecke, P., De Cock, P. & Sunaert, S. (2005) Quantitative diffusion tensor imaging in cerebral palsy due to periventricular white matter injury. *Brain* **128**, 2562–2577.

Thomas, C., Moya, L., Avidan, G., Humphreys, K., Jung, K.J., Peterson, M.A. & Behrmann, M. (2008) Reduction in white matter connectivity, revealed by diffusion tensor imaging, may account for age-related changes in face perception. *J Cogn Neurosci* **20**, 268–284.

Thompson, P.M., Lee, A.D., Dutton, R.A., Geaga, J.A., Hayashi, K.M., Eckert, M.A., Bellugi, U., Galaburda, A.M., Korenberg, J.R., Mills, D.L., Toga, A.W. & Reiss, A.L. (2005) Abnormal cortical complexity and thickness profiles mapped in Williams syndrome. *J Neurosci* **25**, 4146–4158.

Tsang, J.M., Dougherty, R.F., Deutsch, G.K., Wandell, B.A. & Ben-Shachar, M. (2009) Frontoparietal white matter diffusion properties predict mental arithmetic skills in children. *Proc Natl Acad Sci U S A* **106**, 22546–22551.

Vernooij, M.W., Smits, M., Wielopolski, P.A., Houston, G.C., Krestin, G.P. & van der Lugt, A. (2007) Fiber density asymmetry of the arcuate fasciculus in relation to functional hemispheric language lateralization in both right- and left-handed healthy subjects: a combined fMRI and DTI study. *Neuroimage* **35**, 1064–1076.

Wakana, S., Jiang, H., Nagae-Poetscher, L.M., van Zijl, P.C. & Mori, S. (2004) Fiber tract-based atlas of human white matter anatomy. *Radiology* **230**, 77–87.

Woods, R.P., Grafton, S.T., Watson, J.D.G., Sicotte, N.L. & Mazziotta, J.C. (1998) Automated image registration: II. Intersubject validation of linear and nonlinear models. *J Comput Assist Tomo* **22**, 153–165.

Xia, Y., Bettinger, K., Shen, L. & Reiss, A.L. (2007) Automatic segmentation of the caudate nucleus from human brain MR images. *IEEE Trans Med Imaging* **26**, 509–517.

Acknowledgment

This study was supported by Grants P01 HD033113-12 (NICHD) and T32 MH19908.